Effect of grain size on thermoelectric properties of n-type nanocrystalline bismuth-telluride based thin films

著者	Takashiri M, Miyazaki K, Tanaka S, Kurosaki J, Nagai D, Tsukamoto H
journal or publication title	Journal of Applied Physics
volume	104
number	8
page range	084302-1-084302-6
year	2008-10-15
URL	http://hdl.handle.net/10228/1205

doi: 10.1063/1.2990774

Effect of grain size on thermoelectric properties of *n*-type nanocrystalline bismuth-telluride based thin films

M. Takashiri,[1,a)] K. Miyazaki,[2] S. Tanaka,[3] J. Kurosaki,[2] D. Nagai,[3] and H. Tsukamoto[3]
[1]*Research Division, Komatsu Ltd., 1200 Manda, Hiratsuka, Kanagawa 254-8567, Japan*
[2]*Department of Mechanical Engineering, Kyushu Institute of Technology, 1-1 Sensui, Tobata-ku, Kitakyushu Fukuoka 804-8550, Japan*
[3]*Department of Biological Functions and Engineering, Kyushu Institute of Technology, 2-4 Hibikino, Wakamatsu-ku, Kitakyushu Fukuoka 808-0196, Japan*

(Received 17 June 2008; accepted 12 August 2008; published online 16 October 2008)

The effect of grain size on the thermoelectric properties of *n*-type nanocrystalline bismuth-telluride based thin films is investigated. We prepare the nanocrystalline thin films with average grain sizes of 10, 27, and 60 nm by a flash-evaporation method followed by a hydrogen annealing process. The thermoelectric properties, in terms of the thermal conductivity by a differential 3ω method, the electrical conductivity, and the Seebeck coefficient are measured at room temperature and used to evaluate the figure of merit. The minimum thermal conductivity is 0.61 $\mathrm{W\,m^{-1}\,K^{-1}}$ at the average grain size of 10 nm. We also estimate the lattice thermal conductivity of the nanocrystalline thin films and compare it with a simplified theory of phonon scattering on grain boundaries. For nanosized grains, the lattice thermal conductivity of nanocrystalline thin films decreases rapidly for smaller grains, corresponding to the theoretical calculation. The figure of merit is also decreased as the grain size decreases, which is attributed to the increased number of defects at the grain boundaries. © *2008 American Institute of Physics*. [DOI: 10.1063/1.2990774]

I. INTRODUCTION

Thermoelectric materials have been widely investigated for past decades and used for solid-state refrigeration and power conversion. Bismuth-telluride based alloys in particular have high performance near room temperature, which is the important range for most industrial applications.[1,2] The performance of the materials are determined by a figure of merit ZT, which is defined as $ZT=S^2\sigma T/\kappa$, where S is the Seebeck coefficient, σ is the electrical conductivity, κ is the thermal conductivity, and T is the absolute temperature.

In order to obtain a high ZT, thermoelectric materials require a high Seebeck coefficient S, a high electrical conductivity σ, and a low thermal conductivity κ. Among these properties, the reduction of thermal conductivity is thought to be the most effective approach to improve the thermoelectric performance. Recent reports have shown that ZT can be increased in nanostructured thermoelectric materials, and the key reason for the increase in ZT is the reduction of thermal conductivity.[3–7]

Nanocrystalline thermoelectric material is one of the simplest nanostructured materials. The fine-grained materials have a large number of grain boundaries, which enhance the phonon-grain boundary scattering, thus reducing the thermal conductivity. There are some reports of reduced thermal conductivity due to grain boundary scattering.[8–11] However, it is challenging to fabricate thermoelectric materials with nanometer-sized crystal grains because the grains grow significantly during thermal processes, such as sintering or hot pressing. We have previously fabricated nanocrystalline bismuth-telluride-based thin films with the average grain size of 60 nm by a flash-evaporation method and shown the reduction of thermal conductivity.[12]

To further reduce the thermal conductivity of the nanocrystalline bismuth-telluride-based thin films and investigate the effect of grain size on thermoelectric properties, we prepare the nanocrystalline thin films by the flash-evaporation method with an improved annealing condition. The grain size of the thin films is estimated using an x-ray diffraction (XRD) and atomic force microscopy (AFM). The thermoelectric properties, in terms of the electric conductivity, the Seebeck coefficient, and the thermal conductivity, are measured at room temperature. The measured thermal conductivity is divided into the lattice thermal conductivity (κ_l) and electronic thermal conductivity (κ_e). Then we investigate the grain size dependence of the lattice thermal conductivity of the nanocrystalline thin films using a simplified phonon transport model.

II. EXPERIMENTAL

The *n*-type nanocrystalline bismuth-telluride-based thin films were fabricated on glass substrates (Corning 7059) by a flash-evaporation method. The flash-evaporation equipment was described elsewhere.[13] The starting material for the flash-evaporation was *n*-type $Bi_{2.0}Te_{2.7}Se_{0.3}$ spherical powders with average powder size of 200 μm, synthesized by a centrifugal atomization method. Inside the flash-evaporation chamber, the distance between the tungsten boat and the substrate was 200 mm. When the chamber was evacuated to 1.4×10^{-3} Pa, we applied a current of 80 A to the tungsten

[a)]Electronic mail: masayuki_takashiri@komatsu.co.jp.

boat until the substrate temperature reached 200 °C. The thickness of the deposited thin films was approximately 0.7 μm.

The nanocrystalline thin films were then annealed in a hydrogen environment. Samples were placed in an electric furnace that was evacuated to 1.0 Pa and purged five times with high-purity (99.999%) argon gas. Then, the furnace was filled with hydrogen gas at atmospheric pressure, and the hydrogen gas flow rate was maintained at 0.3 slm throughout the annealing process. The temperature was increased steadily at 5 K/min to the set temperature, and the samples were then annealed at the set temperature for 30 min. After annealing, the samples were cooled down naturally to room temperature.

The surface and cross section morphology, crystallinity, and composition of the nanocrystalline thin films were investigated by means of AFM, scanning electron microscopy (SEM), XRD, and energy-dispersive x-ray analysis (EDX). The in-plane electrical conductivity σ of the nanocrystalline thin films was measured at room temperature by a four-point probe method with accuracy of $\pm 3\%$, and the in-plane Seebeck coefficient S was also measured at room temperature with accuracy of $\pm 5\%$.[8] One end of the thin film was connected to a heat sink and the other end to a heater. The Seebeck coefficient was determined as the ratio of the potential difference (ΔV) along the films to the temperature difference (ΔT). The cross-plane thermal conductivity was determined at room temperature by a differential 3ω method with accuracy of $\pm 10\%$.[8] Details of the thermal conductivity measurement and the sample fabrication were described previously.[12,14,15] In brief, a SiO_2 film (0.7 μm thick) was deposited on the thin film with a low deposition rate (0.12 nm/s) by a sputtering method. A thin aluminum wire was deposited on the sample by electron beam evaporation through shadow masks. The thin aluminum wire was 20 μm wide and the length of the heater part was 2 mm. Because the thin film and the SiO_2 film were far thinner than the width of the wire, the direction of heat flow can be considered as perpendicular to the thin film. We also fabricated reference samples that lacked the nanocrystalline thin film but were otherwise identical to the primary samples. The reference samples were used to subtract off the unknown thermal properties of the insulation layers. The figure of merit ZT was estimated from the results of the electrical conductivity, the Seebeck coefficient, and the thermal conductivity.

III. RESULTS AND DISCUSSION

A. Structural properties of nanocrystalline thin films

The surface morphology and the grain structure of the n-type nanocrystalline bismuth-telluride-based thin films are characterized by AFM (Fig. 1). To make the grain structure clear, the grain boundaries are drawn by solid lines on the right half of the images. The as-deposited thin film and the two annealed thin films are all continuous with no porosity. The grain size of the as-deposited thin film is slightly smaller than that of the thin film annealed at 150 °C. As the annealing temperature increases from 150 to 250 °C, the grains grow rapidly but the grain size is still around 100 nm.

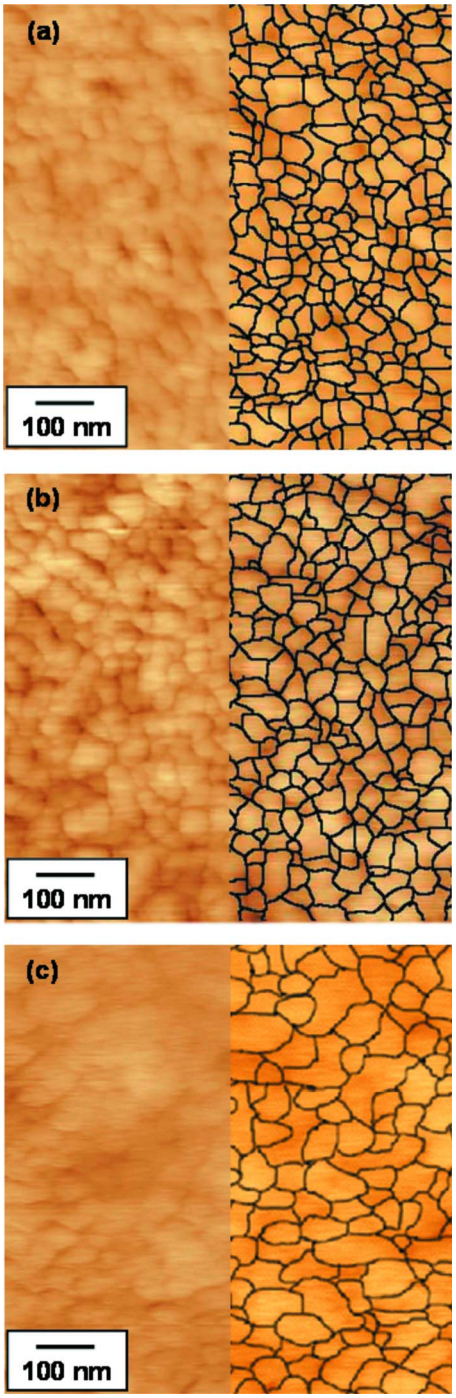

FIG. 1. (Color online) Surface morphology and grain structure of the n-type nanocrystalline bismuth-telluride-based thin films studied by AFM. (a) The as-deposited thin film, (b) the films annealed at 150 °C, and (c) at 250 °C. To make grain structure more clear, the grain boundaries are drawn by solid lines on the right half of the image.

The cross section structure of the nanocrystalline thin films is investigated by means of SEM (Fig. 2). The thickness of all the thin films is approximately 0.7 μm, indicating that any evaporation losses during the annealing process are very small. The grains of the as-deposited thin film are small but still observable at this magnification. At an annealing temperature of 150 °C, the grains of the thin film are slightly larger than those of the as-deposited thin film. The grains of the thin film annealed at 250 °C are much larger. Thus, these

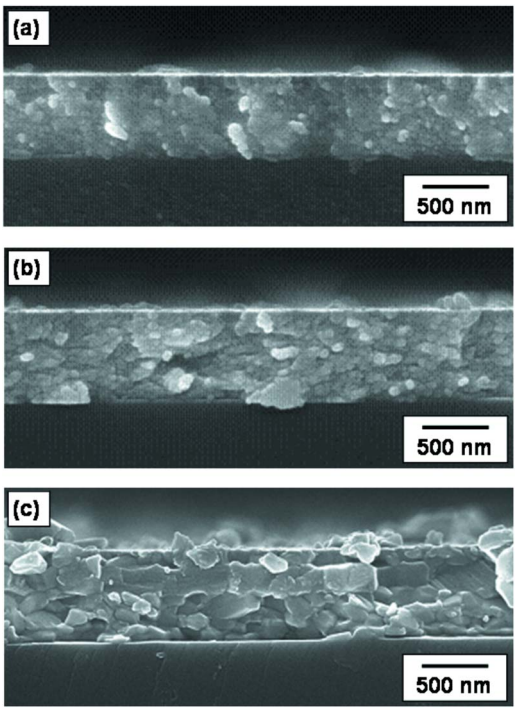

FIG. 2. (Color online) Cross section morphology and grain structure of the *n*-type nanocrystalline bismuth-telluride-based thin films by SEM. (a) The as-deposited thin film, (b) the films annealed at 150 °C and (c) at 250 °C.

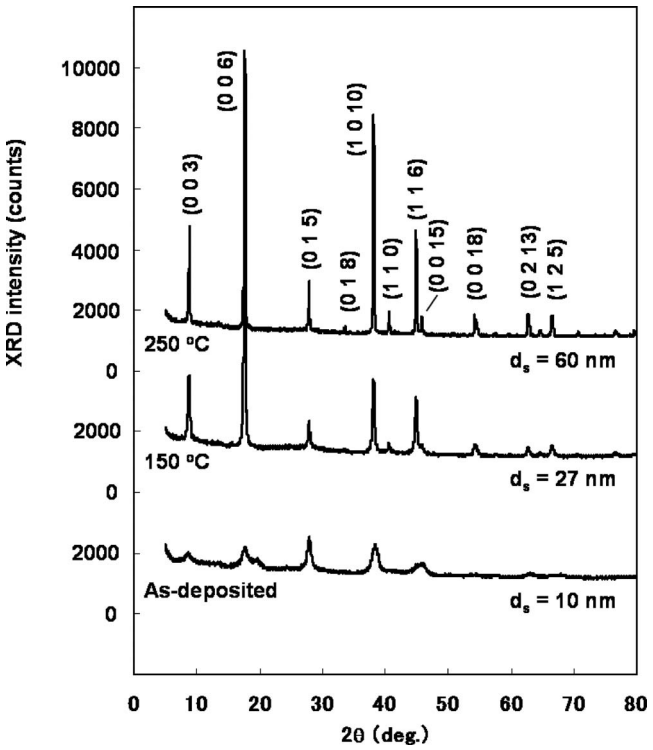

FIG. 3. XRD patterns of the *n*-type nanocrystalline bismuth-telluride-based thin films. The average grain size (d_s) of the thin films is estimated from Scherrer's equation.

phenomena are consistent with the results of surface morphology studied by AFM, and we conclude that the annealing process leads to similar grain growth in both the in-plane and cross-plane directions.

The crystallinity and orientation of the nanocrystalline thin films are investigated by XRD (Fig. 3). The XRD intensity of the thin films is enhanced, and the full-width at half maximum (FWHM) of the XRD peaks is narrowed as the annealing temperature increases. We estimate the average grain sizes of the thin films from the FWHM of the XRD peaks using Scherrer's equation. The grain size of the as-deposited thin film is estimated as 10 nm, and those of the thin films annealed 150 and 250 °C are 27 and 60 nm, respectively. Regarding the crystal orientation of the thin films, the XRD patterns of all of the thin films are found to exhibit multiple peaks, including *c*-axis oriented peaks as well as other oriented peaks. These results indicate that the thin films do not have any preferred crystal orientation.

EDX provides the atomic composition of the initial $Bi_{2.0}Te_{2.7}Se_{0.3}$ powders and of the nanocrystalline thin films as shown in Table I. The composition of the powders is stoichiometric and its as-deposited thin film deviates slightly from stoichiometric, revealing a slightly tellurium-rich structure. The composition of the annealed thin films is almost same as the as-deposited thin films. This indicates that the elements contained in the thin films have hardly evaporated during the annealing process.

B. Effect of grain size on thermal conductivity of nanocrystalline thin films

Figure 4 shows experimentally measured temperature amplitudes experienced by a 20 μm wide heater on both the reference sample and the samples with nanocrystalline thin films. The thermal conductivity of the nanocrystalline thin films is extracted from a curve fit of the measured temperature difference.[16,17] The temperature difference between the reference sample and the as-deposited thin film is the largest among the three samples, while the temperature difference between reference and film is smallest for the thin film annealed at 250 °C.

The thermal conductivities of the *n*-type nanocrystalline bismuth-telluride-based thin films are shown in Table II. For comparison, the corresponding values of the sintered bismuth-telluride bulk material are listed in the table. The electronic thermal conductivity is calculated from the measured electrical conductivity by using the Wiedemann–Franz law, where the Lorenz number is taken to be $L=2.45\times10^{-8}$ W Ω/K^2. The lattice thermal conductivity is estimated by assuming that κ_e is isotropic and subtracting the calculated electronic thermal conductivity from the measured total thermal conductivity (κ_{total}). The cross-plane thermal conductivity of the as-deposited thin film is 0.61 W m^{-1} K^{-1}, and those of the thin films annealed at 150

TABLE I. The atomic composition of the starting powders and resulting thin films, as determined by EDX.

Samples		Bi (at. %)	Te (at. %)	Se (at. %)
Powders		40	54	6
Nanocrystalline bismuth-telluride based thin films	As-deposited	38	56	6
	150 °C	38	57	5
	250 °C	38	57	5

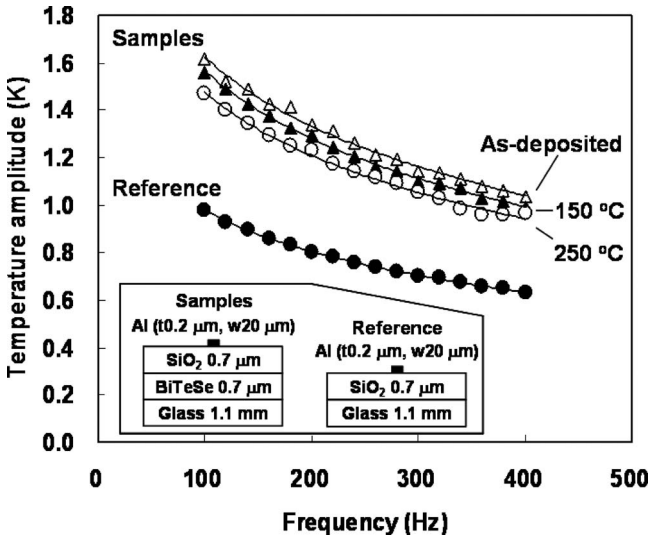

FIG. 4. The temperature amplitudes experienced by 20 μm wide heaters deposited onto the reference and the *n*-type nanocrystalline bismuth-telluride-based thin films.

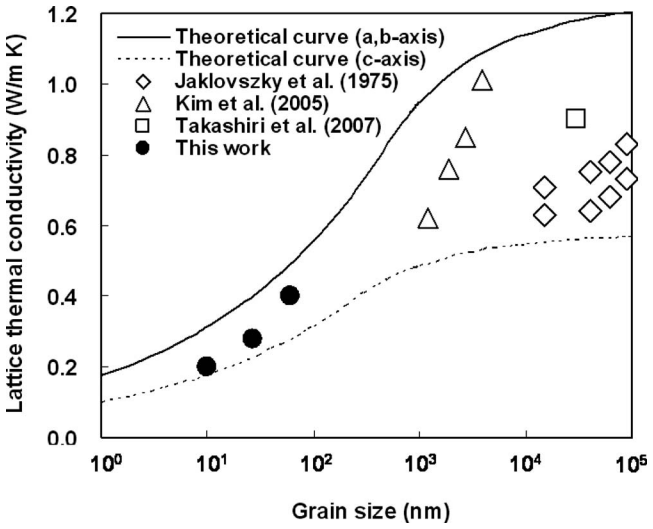

FIG. 5. Lattice thermal conductivity as a function of the grain size of the *n*-type nanocrystalline bismuth-telluride-based thin films and reported experimental results. The solid and dashed lines are the theoretical calculations using a phonon transport model.

and 250 °C are increased to 0.68 and 0.80 W m^{-1} K^{-1}, respectively. Thus, the thermal conductivity of the nanocrystalline thin films is decreased as the grain size decreases. The electronic thermal conductivity (κ_e) of all of the thin films is almost constant at 0.40 W m^{-1} K^{-1} because the electrical conductivity of these samples is nearly constant. The reason for this phenomenon is discussed in Sec. III C. On the other hand, the lattice thermal conductivity of the nanocrystalline thin films decreases as the average grain size is decreased. The grain boundaries in the thin films are more numerous for the smaller grain size, thus reducing the thermal conductivity through increased scattering of phonons on the grain boundaries. The minimum lattice thermal conductivity observed in these samples is 0.20 W m^{-1} K^{-1} at a grain size of 10 nm. Thus, the lattice thermal conductivity is reduced by half compared with its nanocrystalline thin film with a grain size of 50 nm and is reduced by approximately 80% compared with its sintered bulk material with a grain size of 30 μm.[12]

To explore the grain size dependence of the lattice thermal conductivity of the nanocrystalline thin films thoroughly, we verify our experimental results using a simplified theory of phonon scattering on grain boundaries. The detailed theory is described elsewhere.[18–21] In brief, this theory is based on the Debye model for the phonon spectrum and the specific heat. It is supposed that the phonon scattering mechanisms are divided into three frequency regions: boundary scattering at low frequencies, phonon-phonon scattering at intermediate frequencies, and alloy scattering at high frequencies. When the effective grain size d_s is much larger than the phonon mean free path l_t, the lattice thermal conductivity κ_l can be expressed as

$$\kappa_l = \kappa_s - \frac{2}{3}\kappa_0\sqrt{\frac{l_t}{3d_s}}, \tag{1}$$

where κ_s is the lattice thermal conductivity of the solid solution when the grain size is large so as to have negligible boundary scattering, and κ_0 is the lattice conductivity in the absence of alloy scattering that corresponds to l_t. Next, if the effective grain size is comparable or smaller than the phonon mean free path, the lattice thermal conductivity can be expressed as

$$\kappa_l = \left(\frac{2\kappa_s}{3}\right)\left[\left(\frac{3d_s}{l_t}\right)\left(\frac{\kappa_s}{2\kappa_0}\right)^2\right]^{1/4}. \tag{2}$$

Figure 5 shows a comparison of the lattice thermal conductivity of the nanocrystalline thin films with the reported experimental results and the calculated thermal conductivity as given in Table III.[22] For comparison, we have included experimental results on hot-pressed Bi_2Te_3 based bulk alloys fabricated by Kim and Mitani[23] and Jaklovszky *et al.*[24] and a $Bi_{2.0}Te_{2.7}Se_{0.3}$ hot-pressed bulk alloy from our previous study.[12] We calculate the lattice thermal conductivities along the *c*-axis and the basal plane (*a*-*b*-axis). In this calculation,

TABLE II. The grain size and the thermal conductivities of the *n*-type nanocrystalline bismuth-telluride-based thin films and the sintered bulk material.

Samples	Annealing temperature	Average grain size	κ_{total} (W/m K)	κ_e (W/m K)	κ_l (W/m K)
Nanocrystalline bismuth-telluride-based thin films	As-deposited	10 nm	0.61	0.41	0.20
	150 °C	27 nm	0.68	0.40	0.28
	250 °C	60 nm	0.80	0.40	0.40
Sintered bismuth-telluride-based bulk material		30 μm	1.6	0.7	0.9

TABLE III. Approximate parameters used in the calculation of lattice thermal conductivity of bismuth-telluride based alloy.

Orientation	T(K)	κ_0 (W/m K)	κ_s/κ_0	l_t (m)
a-*b*-axis	300	1.5	0.8	2.3×10^{-7}
c-axis	300	0.7	0.8	1.1×10^{-7}

Eq. (1) is employed when d_s is larger than 500 nm, and then Eq. (2) is employed when d_s is smaller than 500 nm. The nanocrystalline thin films do not have any preferred crystal orientation so that the lattice thermal conductivities are presented between the theoretical curves of the *a*-*b*-axis and the *c*-axis. The experimental results show that the lattice thermal conductivity decreases rapidly in the nanosize region of the grain size, corresponding to the theoretical calculation.

C. Thermoelectric properties of nanocrystalline thin films

The thermoelectric properties of *n*-type nanocrystalline bismuth-telluride-based thin films are presented in Table IV. For comparison, the corresponding values of the sintered bismuth-telluride bulk material are also listed in the table. The electrical conductivities of all the thin films are around 5.4×10^4 S/m. On the other hand, the Seebeck coefficient of the as-deposited thin film is −58.0 μV/K, and then the absolute value of the Seebeck coefficient is increased as the annealing temperature increases. Finally, the Seebeck coefficient of the thin film annealed at 250 °C reaches −186.1 μV/K, which is approximately same value as its typical bulk alloys.

The correlation between the annealing temperature dependence of the electrical conductivity and the Seebeck coefficient is complicated. It is easy to understand the case that the electrical conductivity is increased and the Seebeck coefficient is kept constant as the annealing temperature increases, corresponding to the increasing the grain size of the thin films. This is because the mobility is enhanced by reducing the carrier scattering on the grain boundaries as the grains grow. However, our results show a different phenomenon. We may consider that a large number of defects exist at the grain boundaries of the as-deposited thin films. The defects act as donors, so that the carrier concentration is enhanced, while at the same time the grain boundaries decrease the mobility by scattering the carriers.[25] Thus, we suggest that the electrical conductivity remains constant as the grains grow because the decreased carrier concentration is approximately compensated for the increased mobility. On the other hand, the Seebeck coefficient is increased as the grains grow. This is because the Seebeck coefficient depends on the carrier concentration, not on the mobility, so that the Seebeck coefficient is increased as the carrier concentration decreases, corresponding to growing the grains.[26]

To estimate the dimensionless figure of merit, the in-plane thermal conductivity of the nanocrystalline thin films is assumed to be identical to that of the cross-plane direction. The figure of merit of the as-deposited thin film and the thin films annealed at 150 and 250 °C is estimated to be ZT =0.19, 0.46, and 0.70, respectively. This indicates that the figure of merit is decreased as the grain size of the thin films decreases.

Therefore, nanocrystalline thin films with high performance by reducing the grain size have not achieved yet in this material system. However, the results of this study are useful to link the enhancement of the thermoelectric properties to the structure of the nanocrystalline thin films. The reduction of the grain size successfully reduces the lattice thermal conductivity, but it also increases the defect density at the grain boundaries, with the net result that the thermoelectric figure of merit is not improved. In order to improve the thermoelectric performance, it is necessary to create the clean grain boundaries while maintaining the nanosize crystal grains. Poudel *et al.* have achieved high thermoelectric performance using nanostructured bismuth antimony telluride bulk alloys with clean grain boundaries.[27] Similarly, for our flash-evaporation method, we think that it is possible to fabricate the nanocrystalline thin films with clean grain boundaries by modifying the deposition equipment and conditions.

IV. CONCLUSION

We investigate the effect of grain size on the thermoelectric properties of *n*-type nanocrystalline bismuth-telluride-based thin films. The nanocrystalline thin films with the average grain of 10, 27, and 60 nm are prepared by a flash-evaporation method followed by a hydrogen annealing process. All the nanocrystalline thin films are flat with fine grain structure, no preferred crystal orientation, and slightly tellurium rich composition. The cross-plane thermal conductivity of the nanocrystalline thin films is measured by a differential 3ω method at room temperature. The in-plane electrical conductivity and Seebeck coefficient are also investigated. The minimum cross-plane thermal conductivity of the nanocrystalline thin films is 0.61 W m^{-1} K^{-1} at the average grain size of 10 nm, and then it is increased up to 0.80 W m^{-1} K^{-1} as the grain size increases to 60 nm. To

TABLE IV. The thermoelectric properties of the *n*-type nanocrystalline bismuth-telluride-based thin films and the sintered bulk material.

Sample	Annealing temperature	κ_{total} (W/m K)	σ (S/m)	S (μV/K)	ZT (300 K)
Nanocrystalline bismuth-telluride-based thin films	As-deposited	0.61	5.5×10^4	−84.0	0.19
	150 °C	0.68	5.4×10^4	−138.1	0.46
	250 °C	0.80	5.4×10^4	−186.1	0.70
Sintered bismuth-telluride-based bulk material		1.6	9.3×10^4	−177.5	0.6

explore the grain size dependence of the thermal conductivity of the nanocrystalline thin films thoroughly, we estimate the lattice thermal conductivity and compare it to a simplified theory of phonon scattering on grain boundaries. The lattice thermal conductivity of nanocrystalline thin films is decreased rapidly in the nanosize region of the grain size, corresponding to the theoretical calculation. Assuming that the in-plane thermal conductivity of the nanocrystalline thin films is identical to that of the cross-plane direction, the figure of merit of the thin film with the grain size of 60 nm is 0.70, and then it becomes 0.19 as the grain size decreases to 10 nm. The reduction of the grain size reduces the lattice thermal conductivity but it also increases the defect density at the grain boundaries, such that the overall thermoelectric performance is degraded. In order to improve the thermoelectric performance, it is necessary to create the clean grain boundaries while maintaining the nanosize crystal grains by modifying the deposition equipment and conditions.

ACKNOWLEDGMENTS

The authors wish to thank Professor Dames at the University of California, Riverside for valuable comments, Dr. Jacquot at Fraunhofer Institut Physikalische Messtechnik in Germany for experimental support, and the staff of the Analysis and Measurement Group at Komatsu Ltd. for technical support.

[1]S. Murata, H. Nakada, T. Abe, H. Tanaka, and A. Watabe, Jpn. J. Appl. Phys., Part 1 **32**, 5284 (1993).
[2]M. Kishi, H. Nemoto, T. Hamao, M. Yamamoto, S. Sudou, M. Mandai, and S. Yamamoto, Proceedings of the 18th International Conference on Thermoelectrics (IEEE, New York, 1999), p. 301.
[3]R. Venkatasubramanian, E. Siivola, T. Colpitts, and B. O'Quinn, Nature (London) **413**, 597 (2001).
[4]T. C. Harman, P. J. Taylor, M. P. Walsh, and B. E. LaForge, Science **297**, 2229 (2002).
[5]K. F. Hsu, S. Loo, F. Guo, W. Chen, J. S. Dyck, C. Uher, T. Hogan, E. K. Polychroniadis, and M. G. Kanatzidis, Science **303**, 818 (2004).
[6]W. Kim, J. Zide, A. Gossard, D. Klenov, S. Stemmer, A. Shakouri, and A. Majumdar, Phys. Rev. Lett. **96**, 045901 (2006).
[7]X. Tang, W. Xie, H. Li, W. Zhao, Q. Zhang, and M. Niino, Appl. Phys. Lett. **90**, 012102 (2007).
[8]M. Takashiri, T. Borca-Tasciuc, A. Jacquot, K. Miyazaki, and G. Chen, J. Appl. Phys. **100**, 54315 (2006).
[9]D. M. Rowe and V. S. Shukla, J. Appl. Phys. **52**, 7421 (1981).
[10]K. Watari, K. Hirano, M. Toriyama, and K. Ishizaki, J. Am. Ceram. Soc. **82**, 777 (1999).
[11]N. Savvides and H. J. Goldsmid, J. Phys. C **13**, 4657 (1980).
[12]M. Takashiri, M. Takiishi, S. Tanaka, K. Miyazaki, and H. Tsukamoto, J. Appl. Phys. **101**, 074301 (2007).
[13]M. Takashiri, T. Shirakawa, K. Miyazaki, and H. Tsukamoto, J. Alloys Compd. **441**, 246 (2007).
[14]T. Borca-Tasciuc, A. R. Kumar, and G. Chen, Rev. Sci. Instrum. **72**, 2139 (2001).
[15]A. Jacquot, B. Lenoir, A. Dauscher, M. Stölzer, and J. Meusel, J. Appl. Phys. **91**, 4733 (2002).
[16]D. G. Cahill, M. Katiyar, and J. R. Abelson, Phys. Rev. B **50**, 6077 (1994).
[17]Y. S. Ju, K. Kurabayashi, and K. E. Goodson, Thin Solid Films **339**, 160 (1999).
[18]H. J. Goldsmid and A. W. Penn, Phys. Lett. **27A**, 523 (1968).
[19]D. M. Rowe *et al.*, *CRC Handbook of Thermoelectrics*, edited by D. M. Rowe (CRC, Boca Raton, FL, 1995).
[20]H. J. Goldsmid, H. B. Lyon, Jr., and E. H. Volckmann, Proceedings of the 14th International Conference on Thermoelectrics (IEEE, New York, 1995), p. 16.
[21]J. W. Sharp and H. J. Goldsmid, Proceedings of the 18th International Conference on Thermoelectrics (IEEE, New York, 1999), p. 709.
[22]G. S. Nolas, J. Sharp, and H. J. Goldsmid, *Thermoelectrics* (Springer, Berlin, 2001).
[23]D.-H. Kim and T. Mitani, J. Alloys Compd. **399**, 14 (2005).
[24]J. Jaklovszky, R. Ionescu, N. Nistor, and A. Chiculita, Phys. Status Solidi A **27**, 329 (1975).
[25]M. Takashiri, T. Shirakawa, K. Miyazaki, and H. Tsukamoto, Trans. Jpn. Soc. Mech. Eng., Ser. A **72**, 1793 (2006) (in Japanese).
[26]A. F. Ioffe, *Semiconductor Thermoelements and Thermoelectric Cooling* (Infosearch, London, 1960).
[27]B. Poudel, Q. Hao, Y. Ma, Y. Lan, A. Minnich, B. Yu, X. Yan, D. Wang, A. Mute, D. Vashaee, J. Liu, M. S. Dresselhaus, G. Chen, and Z. Ren, Science **320**, 634 (2008).